Low Temperature Physics ARTICLE scitation.org/journal/ltp

Multi-signal spectroscopy of qubit-resonator systems

Cite as: Fiz. Nizk. Temp. **47**, 414–419 (May 2021); doi: 10.1063/10.0004230
Submitted: 22 March 2021

M. A. Nakonechnyi,[1,a)] D. S. Karpov,[1] A. N. Omelyanchouk,[1] and S. N. Shevchenko[1,2]

AFFILIATIONS

[1]B. Verkin Institute for Low Temperature Physics and Engineering of the National Academy of Sciences of Ukraine, Kharkiv 61103, Ukraine
[2]V. N. Karazin Kharkov National University, Kharkov 61022, Ukraine

[a)]**Author to whom correspondence should be addressed:** mykhail.nakonechnyi@gmail.com

ABSTRACT

Some unique properties of superconducting devices are promising for the development of modern quantum technologies. Superconducting quantum circuits use large coupling constants and provide good scalability and controllability due to their macroscopic dimensions. Still, micro-fabrication methods have some hardship with reproducibility of identical superconducting quantum circuits. The dressed state approach presents some possibility to reduce influence of non-identity of qubits. We study a qubit-resonator system, when the qubit interacts with three signals. Such system configuration adds additional flexibility for circuit tunability. A particular realization of such a system is a superconducting flux qubit coupled to a transmission-line resonator driven by three signals. We describe this triply-driven system in terms of the dressed qubit states and conclude that using several signals can be beneficial for both system spectroscopy and tunability. Such study of a qubit-based system, coupled to both classical and quantum fields, can be useful for detection of individual itinerant microwave photons.

1. INTRODUCTION

Superconducting quantum systems have a number of important advantages that make them a promising platform for modern quantum technologies.[1–3] Due to their macroscopic size, they provide good scalability as well as controllability. Although the first experiments in circuit electrodynamics focused on demonstrating fundamental quantum effects, the emphasis has now shifted to creating hybrid structures for modeling quantum information protocols.[4] In addition to decoherence, inaccuracies in manufacturing of samples and their non-identity remain significant obstacles in the study of multicomponent schemes. To avoid such side effects, we suggest one of the tools, which consists of using the qubit dressed model.

The notion of dressed states is important for various effects, such as Autler–Townes effect,[5,6] electromagnetically induced transparency,[7] multi-photon transitions,[8–11] cooling,[12] Landau-Zener-Stuckelberg-Majorana interferometry,[13–16] lasing,[17] Mollow triplet.[18] One important conclusion, which one can draw from studying dressed states, is that adding one more signal allows for such fine tuning which would not be accessible otherwise (with single dressing field).[19,20] A flux qubit was considered in a qubit-resonator system, and the transmission coefficient of an electromagnetic wave was obtained.[21] Then, in Ref. 22, a doubly-driven system was described in terms of doubly-dressed states of a qubit, which was proposed to be used to create quantum amplifiers.[23–25] Similar experiments[26] showed amplification and attenuation of the probe signal for two different types of superconducting qubits: a flux qubit based on a loop with three Josephson junctions and a phase-slip qubit.

In our work, we consider a superconducting flux qubit coupled to a transmission-line resonator, which system is being driven with three signals. For the experimental formulation of the problem see Ref. 27, while in the theoretical formulation we are following Ref. 28. In Ref. 27, the effect of a strong nonresonant control signal on the energy levels for a flux qubit was considered. The authors observed a change in the energy levels of a qubit by a dynamic Stark shift caused by a driving signal. A similar work[29] investigated the response of a qubit and the formation of dressed states with three states; our model brings more details to these processes.

The formulation of the problem for a qubit-resonator system with both classical and quantum signals is important for detection

of itinerant microwave photons.[30,31] Indeed, such photons, described by the quantum field, can route via the transmission line. Then, these meet the qubit-cavity system, of which the dressed energy levels can be fine-tuned. Consequently, the observed transmission coefficient provides the tool to probe individual photons. The aim of our present work is the detailed study of such dressed states in the triply-driven qubit-resonator system.

The rest of the paper is organised as follows. In Sec. 2 we present our model and introduce the Hamiltonian of the system. Making use of the rotating-wave approximation results in the dressed states, as described in Sec. 3 with the details in the Appendix. In Sec. 4 we discuss the resonant transmission through the system qubit-resonator and describe the position of the resonances. The paper ends with the Conclusions.

2. HAMILTONIAN

The system which we consider consists of a qubit and a resonator with three signals. To be more specific, we consider a flux qubit coupled to a transmission-line resonator, as shown in Fig. 1.

Consider a qubit that interacts with three resonator signals: two classical (with frequencies ω_d and ω_s and amplitudes A_d and B_s) and one quantum (with the frequency ω_p and the amplitude ξ_p). Amplitudes are related as: $\xi_p < A_\mathrm{d}$, B_s. The Hamiltonian of the system has the following form:[28]

$$H = H_\mathrm{qb} + H_r + H_\mathrm{probe} + H_\mathrm{drive} + H_{sd} + H_\mathrm{int.} \tag{1}$$

Here, the Hamiltonian consists of the following parts. The qubit is described by

$$H_\mathrm{qb} = \frac{\hbar\omega_\mathrm{qb}}{2}\sigma_z \tag{2}$$

with the energy difference $\hbar\omega_\mathrm{qb} = \sqrt{\varepsilon_0^2 + \Delta^2}$, the energy bias ε_0, which is defined by the external magnetic flux, minimal energy splitting Δ, and the Pauli matrices σ_i. Note that this is given in the representation of the qubit energy eigenstates. Next, the resonator is characterized by the resonant frequency ω_r, and the annihilation/creation operators $a/a^\dagger$:

$$H_r = \hbar\omega_r a^\dagger a. \tag{3}$$

The probe field with the amplitude ξ_p and the frequency ω_p is described by

$$H_\mathrm{probe} = \hbar\xi_p(a e^{i\omega_p t} + a^\dagger e^{-i\omega_p t}). \tag{4}$$

The probe field is supplied via the transmission line. In contrast, the next, driving, signal is supplied through the magnetic flux[21]

$$H_\mathrm{drive} = A_d \cos\omega_d t\tilde{\sigma}_z', \quad \tilde{\sigma}_z' = \left(\frac{\varepsilon_0}{\hbar\omega_\mathrm{qb}}\sigma_z + \frac{\Delta}{\hbar\omega_\mathrm{qb}}\sigma_x\right). \tag{5}$$

Note that the former signal is described by the cavity operators, while the latter is defined by the qubit operators. Finally, the third (strong) driving signal enters with the Hamiltonian

$$H_{sd} = B_s \cos\omega_s t\tilde{\sigma}_z'. \tag{6}$$

So, it is the first (weak) signal which is considered fully quantum-mechanically, while the second and the third (strong) signals are considered semiclassically. Finally, the interaction of the qubit and the resonator (with the coupling constant g) is given by the term

$$H_\mathrm{int} = g(a + a^\dagger)\tilde{\sigma}_z'. \tag{7}$$

With the Hamiltonian (1) one can describe both the eigenstates and dynamics of a qubit coupled to a resonator with three signals.

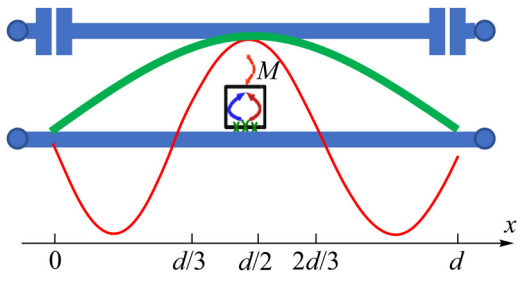

FIG. 1. Schematic diagram of a driven qubit-resonator system. The qubit is a flux qubit, which is a superconducting ring with three Josephson junctions; the current in the loop can be in either direction, which defines the qubit basis; the loop is pierced by the external magnetic flux, which defines both the energy bias and the driving. A resonator is based on a transmission line interrupted by two capacitors. The qubit is coupled to the resonator via mutual inductance M. The transmission line is excited by two signals, corresponding to first and third harmonics of the resonator; distribution of the current density is given by the green and red lines, respectively. The qubit is situated at the maxima of the current densities, at $x = d/2$.

3. DRESSED AND DOUBLY-DRESSED STATES

Now, in order to describe our system with three drive signals, we can make use of the rotating-wave approximations (RWA) so that to exclude the respective time dependence from the Hamiltonian. The result is known as dressed states. Details of using RWA corresponding to the three signals are given in the Appendix. Essentially, each time excluding the signal from the Hamiltonian, starting from the bare energy levels, we obtain dressed and doubly-dressed energy levels with the respective energy separations:

$$\hbar\omega_\mathrm{qb} = \sqrt{\Delta^2 + \varepsilon_0^2} \tag{8}$$

for the bare states, which are controlled by the energy bias ε_0;

$$\Delta\bar{E} = \sqrt{\tilde{\Delta}^2 + \tilde{\varepsilon}^2} \tag{9}$$

for the dressed states, with $\tilde{\Delta} = A_d\Delta/\hbar\omega_\mathrm{qb}$ and $\tilde{\varepsilon} = \hbar(\omega_\mathrm{qb} - \omega_d)$, which are controlled by the driving signal with the frequency ω_d

and amplitude A_d; and

$$\Omega_{qb} = \sqrt{\Lambda^2 + \delta\omega_{qb}^2}, \tag{10}$$

for the doubly-dressed states, with $\delta\omega_{qb} = (\Delta\tilde{E}/\hbar) - \omega_s$, and $\Lambda = B_s(\varepsilon_0/\hbar\omega_{qb})(\tilde{\Delta}/\Delta\tilde{E})$, which are then controlled by the signal with the frequency ω_s, and amplitude B_s.

Taking into account the third, probe, signal with the frequency ω_p and amplitude ξ_p brings us to the Hamiltonian in the form of the well-known Janes–Cummings Hamiltonian:

$$\tilde{H}_{RWA-3} = \hbar\frac{\delta\tilde{\omega}_{qb}}{2}\tilde{\sigma}_2' + \hbar\delta\omega_r a^\dagger a + \tilde{\gamma}(a\tilde{\sigma}_+' + a^\dagger\tilde{\sigma}_-') + \hbar\xi_p(a + a^\dagger), \tag{11}$$

where

$$\delta\tilde{\omega}_{qb} = \Omega_{qb} - \omega_p, \quad \tilde{\gamma} = \gamma\frac{\Delta}{\Omega_{qb}}, \quad \delta\omega_r = \omega_r - \omega_p.$$

Expression (11) coincides exactly with the Hamiltonian of an effective two-level system interacting with a quantum field. But now we have the opportunity to influence the shape of the levels by changing the parameters of the excitation fields. The first term in Eq. (11) gives the energy levels of the triply-dressed states.

The bare, dressed, and doubly-dressed energy levels are shown in Fig. 2. For calculations we take the parameters close to the ones in Ref. 27: $\Delta/h = 2.97$ GHz, $\omega_r/2\pi = 2.59$ GHz, $\omega_p = \omega_r$, $\omega_d = 3\omega_r$, $\omega_s/2\pi = 2.62$–3.25 GHz, $g/h = 3$ MHz. So, the position of the resonances in the transmission coefficient can be used for defining the dressed-energy spectra of the system, which can be used for the multi-signal spectroscopy.[27,32]

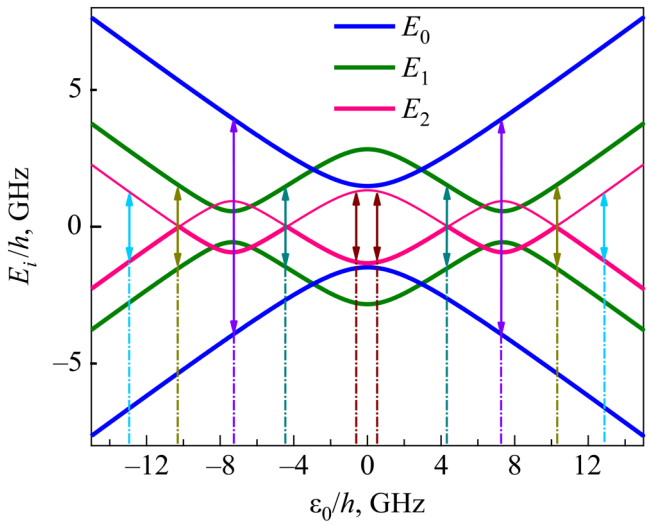

FIG. 2. Energy levels of a triply-driven qubit. The bare energy levels, $E_0 = \pm\hbar\omega_{qb}/2$, are shown with the blue lines; the dressed levels, $E_1 = \pm\Delta\tilde{E}/2$, are shown with the green line; the doubly-dressed levels, $E_2 = \pm\hbar\Omega_{qb}/2$, are shown with the pink lines. The arrows have the length corresponding to the frequencies $\omega_d/2\pi = 7.77$ GHz, $\omega_p/2\pi = 2.59$ GHz, $\omega_s/2\pi = 3.0$ GHz. Where the energy levels are matched by the photon energy, we expect the resonant excitation of the qubit-resonator system, resulting in the changes of the transmission coefficient. Position of the resonances, at $\varepsilon_0 = \varepsilon_0^*$, we further demonstrate in Fig. 3. The structure of the energy levels and the position of the resonances are defined by the driving amplitudes; here we take these: $A_d/h = 3$ GHz and $B_s/h = 1$ MHz.

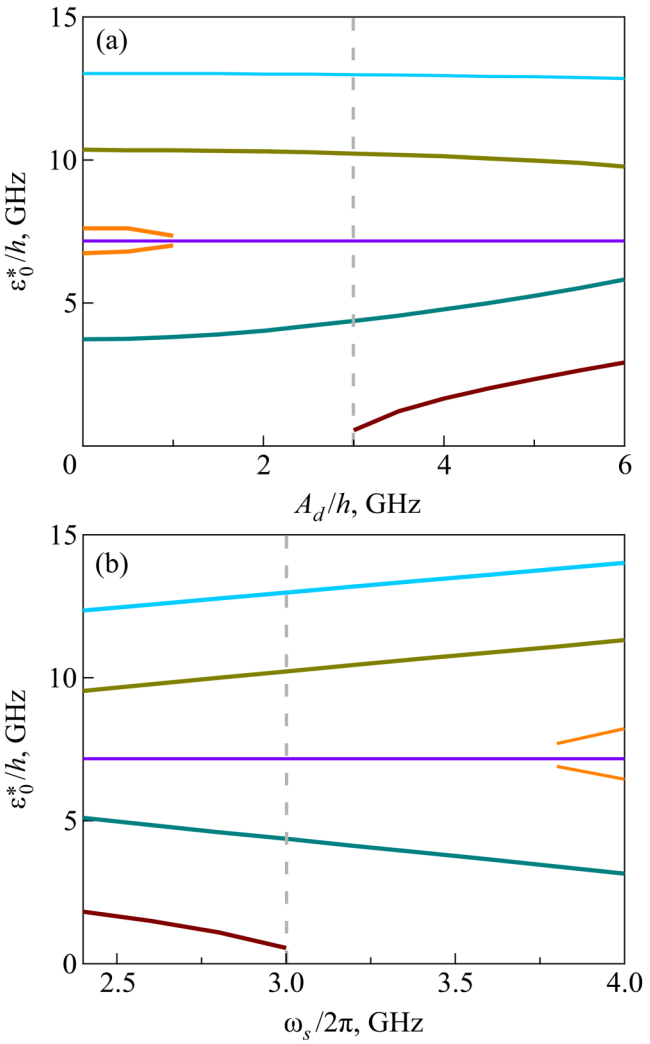

FIG. 3. Position of the resonances ε_0^* as a function of the driving amplitude A_d (a) and the varying second signal frequency ω_s (b). The colours of the lines correspond to their position shown by the vertical dashed lines in Fig. 2. Also here the vertical gray lines show the values of A_d and ω_s, at which Fig. 2 was plotted. For calculations we took: $B_s = 1$ GHz, $\omega_s/2\pi = 3$ GHz in (a) and $A_d/h = 3$ GHz in (b).

4. RESONANT TRANSMISSION

When a qubit is coupled to a resonator, the state of such qubit-resonator system is usually probed via either reflection or transmission of a probe signal.[20,27,33] In the multiple-signal formulation, we expect resonances at positions where respective energy levels are matched by an excitation-signal frequency. Physically, this is analogous to the phenomena known as the electromagnetically induced transparency.[7,34] In particular, we expect the resonances at where the bare levels are matched by the first driving signal

$$\omega_{\rm qb}(\varepsilon_0) = \omega_d, \tag{12}$$

where the dressed energy levels are matched by the second driving signal

$$\Delta\tilde{E}(\varepsilon_0) = \hbar\omega_s, \tag{13}$$

and where the doubly-dressed states are matched by the probe signal

$$\Omega_{\rm qb}(\varepsilon_0) = \omega_p. \tag{14}$$

The position of the respective resonances are shown by the arrows in Fig. 2. Next, we present the position of the possible resonances in Fig. 3. There, the lines show the solution of Eq. (12)–(14). Multiple resonances and there dependence on the driving parameters helps understanding of resonant transmission in the experiments like Ref. 27.

5. DISCUSSION AND CONCLUSIONS

We have described theoretically the qubit-resonator system, when a qubit interacts with three signals. We have shown that a strong excitation signal can be used to control the energy levels of a qubit-based system by several parameters, such as the amplitudes and frequencies of the signals. The ability to regulate energy levels in this way stems from their interaction with the driving fields. We have shown that a qubit interacting with several signals can still be described as an effective quantum two-level system, in terms of dressed states. Importantly, such energy levels are highly tunable by the dressing signals. Probing the energy levels of the systems can be useful for the system spectroscopy. On the other hand, measuring the resonant transmission can be used for detecting itinerant photons of the probe field.

ACKNOWLEDGMENTS

We thank E. V. Il'ichev, G. Oelsner, and O. G. Turutanov for fruitful discussions and O. V. Ivakhnenko for the help with the graphs. The authors acknowledge partial support by the Grant of the President of Ukraine (Grant No. F84/185-2019), NATO SPS Programme (Grant No. G5796), NAS of Ukraine target program "Prospective basic research and innovative development of nanomaterials and nanotechnologies for the needs of industry, healthcare, and agriculture."

APPENDIX: ROTATING-WAVE TRANSFORMATIONS

In this Appendix we consider three times rotating-wave approximations (RWA) so that to exclude driving and obtain dressed states.

Rotating-wave approximation 1

Consider first the full Hamiltonian H, Eq. (1) and let us make the unitary transformation

$$U_1 = \exp(i\omega_d t\sigma_z/2). \tag{A1}$$

Then, after simplification we obtain the following expression

$$\begin{aligned}\tilde{H}_{RWA-1} &= U_1 H U_1^\dagger + i\hbar\dot{U}_1 U_1^\dagger = \tilde{H}_0 + \tilde{H}(t)\\ &= \frac{\tilde{\varepsilon}}{2}\sigma_z + \frac{\tilde{\Delta}}{2}\sigma_x + \hbar\omega_r a^\dagger a + \tilde{g}(a + a^\dagger)\sigma_z\\ &\quad + \hbar\xi_p(ae^{i\omega_p t} + a^\dagger e^{-i\omega_p t}) + B_s\cos\omega_s t\frac{\varepsilon_0}{\omega_{\rm qb}}\sigma_z,\end{aligned} \tag{A2}$$

where

$$\tilde{\Delta} = \frac{A_d\Delta}{\hbar\omega_{\rm qb}}, \quad \tilde{\varepsilon} = \hbar(\omega_{\rm qb} - \omega_d), \quad \tilde{g} = g\frac{\varepsilon_0}{\hbar\omega_{\rm qb}}. \tag{A3}$$

Now we rewrite the Hamiltonian in the eigenbasis of $\tilde{H}_0$ xwith the unitary transformation $S_1 = \exp(i\tau\sigma_y/2)$, where $\tan\tau = -\tilde{\Delta}/\tilde{\varepsilon}$, and obtain

$$\tilde{H}_1 = \frac{\Delta\tilde{E}}{2}\tilde{\sigma}_z + B_s\cos\omega_s t\frac{\varepsilon_0}{\hbar\omega_{\rm qb}}\sigma_z + \tilde{g}(a + a^\dagger)\sigma_z, \tag{A4}$$

with $\Delta\tilde{E} = \sqrt{\tilde{\Delta}^2 + \tilde{\varepsilon}^2}$ and

$$\sigma_z = \cos\tau\tilde{\sigma}_z + \sin\tau\tilde{\sigma}_x = \frac{\tilde{\varepsilon}}{\Delta\tilde{E}}\tilde{\sigma}_z - \frac{\tilde{\Delta}}{\Delta\tilde{E}}\tilde{\sigma}_x.$$

Rotating-wave approximation 2

As a following step, we make the unitary transformation with respect to the signal with the frequency ω_s:

$$U_2 = \exp(i\omega_s t/\tilde{\sigma}_z/2). \tag{A6}$$

Then, after applying this transformation, we obtain the Hamiltonian in the form

$$\begin{aligned}\tilde{H}_1' &= \frac{\Delta\tilde{E} - \hbar\omega_s}{2}\tilde{\sigma}_z + \frac{B_z}{2}\frac{\varepsilon_0}{\omega_{\rm qb}}\\ &\quad\times\left[(e^{i\omega_s t} + e^{-i\omega_s t})\frac{\tilde{\varepsilon}}{\Delta\tilde{E}}\tilde{\sigma}_z - \frac{\tilde{\Delta}}{\Delta\tilde{E}}(e^{-2i\omega_s t}\tilde{\sigma}_+ + e^{2i\omega_s t}\tilde{\sigma}_- + \tilde{\sigma}_x)\right]\\ &\quad + \tilde{g}(a + a^\dagger)\left[\frac{\tilde{\varepsilon}}{\Delta\tilde{E}}\tilde{\sigma}_z - \frac{\tilde{\Delta}}{\Delta\tilde{E}}(e^{-i\omega_s t}\tilde{\sigma}_+ + e^{i\omega_s t}\tilde{\sigma}_-)\right].\end{aligned} \tag{A7}$$

Then the Hamiltonian of the system takes the form

$$\begin{aligned}\tilde{H}_{RWA-2} &= \frac{\delta\omega_{\rm qb}}{2}\tilde{\sigma}_z - \frac{\Delta}{2}\tilde{\sigma}_z + g(a + a^\dagger)\tilde{\sigma}_z + \hbar\omega_r a^\dagger a\\ &\quad + \hbar\xi_p(ae^{i\omega_p t} + a^\dagger e^{-i\omega_p t}),\end{aligned} \tag{A8}$$

where

$$\delta\omega_{qb} = \frac{\Delta\tilde{E}}{\hbar} - \omega_s, \Lambda = B_s \frac{\varepsilon_0}{\hbar\omega_{qb}} \frac{\tilde{\Delta}}{\Delta\tilde{E}}, \gamma = \tilde{g}\frac{\tilde{\varepsilon}}{\Delta\tilde{E}}. \quad \text{(A9)}$$

In the eigenbasis of the time-independent Hamiltonian, using the transformation

$$S_2 = \exp(i\zeta\tilde{\sigma}_y/2), \quad \tan\zeta = \Lambda/\delta\omega_{qb}, \quad \text{(A10)}$$

the expression (A8) takes the following form

$$\tilde{H}'_{RWA-2} = \frac{\Omega_{qb}}{2}\tilde{\sigma}'_z + \gamma(a + a^\dagger)\tilde{\sigma}_z + \hbar\omega_r a^\dagger a + \hbar\xi_p(ae^{i\omega_p t} + a^\dagger e^{-i\omega_p t}), \quad \text{(A11)}$$

with

$$\Omega_{qb} = \sqrt{\Lambda^2 + \delta\omega_{qb}^2}, \quad \text{(A12)}$$

and

$$\tilde{\sigma}_z = \cos\varsigma\tilde{\sigma}'_z + \sin\varsigma\tilde{\sigma}'_x = \frac{\delta\omega_{qb}}{\Omega_{qb}}\tilde{\sigma}'_z + \frac{\Lambda}{\Omega_{qb}}\tilde{\sigma}'_x \quad \text{(A13)}$$

Rotating-wave approximation 3

Finally, we make the unitary transformation

$$U_3 = \exp(i\omega_p t(a^\dagger a + \tilde{\sigma}'_z/2)). \quad \text{(A14)}$$

After this, the expression (A11) results in the complete Hamiltonian of the system in the form

$$\tilde{H}_{RWA-3} = \hbar\frac{\delta\tilde{\omega}_{qb}}{2}\tilde{\sigma}'_z + \tilde{\gamma}(a\tilde{\sigma}'_+ + a^\dagger\tilde{\sigma}'_-) + \hbar\delta\omega_r a^\dagger a + \hbar\xi_p(a + a^\dagger), \quad \text{(A15)}$$

where

$$\delta\tilde{\omega}_{qb} = (\Omega_{qb} - \omega_p), \quad \tilde{\gamma} = \gamma\frac{\Delta}{\Omega_{qb}}, \quad \delta\omega_r - \omega_p. \quad \text{(A16)}$$

We further analyze this Hamiltonian as well as the dressed states in the main text.

REFERENCES

[1]J. Q. You and F. Nori, Nature **474**, 589 (2011).
[2]X. Gu, A. F. Kockum, A. Miranowicz, Y.-X. Liu, and F. Nori, Phys. Rep. **718–719**, 1 (2017).
[3]S. N. Shevchenko, *Mesoscopic Physics Meets Quantum Engineering* (World Scientific, Singapore, 2019).
[4]Z.-L. Xiang, S. Ashhab, J. Q. You, and F. Nori, Rev. Mod. Phys. **85**, 623 (2013).
[5]M. Yan, E. G. Rickey, and Y. Zhu, Phys. Rev. A **64**, 013412 (2001).
[6]J. Pan, Y. Fan, Y. Li, X. Dai, X. Wei, Y. Lu, C. Cao, L. Kang, W. Xu, J. Chen, G. Sun, and P. Wu, Phys. Rev. B **96**, 024502 (2017).
[7]L. Chang-Biao, N. Zhi-Qiang, Z. Wei-Feng, Z. Yan-Peng, S. Jian-Ping, L. Yuan-Yuan, and L. Ke-Qing, Chin. Phys. Lett. **25**, 4266 (2008).
[8]A. P. Saiko and R. Fedaruk, JETP Lett. **91**, 681 (2010).
[9]A. P. Saiko, R. Fedaruk, and S. A. Markevich, J. Phys. B **47**, 155502 (2014).
[10]A. P. Saiko, R. Fedaruk, and S. A. Markevich, J. Mag. Res. **259**, 47 (2015).
[11]A. P. Saiko, S. A. Markevich, and R. Fedaruk, Phys. Rev. A **98**, 043814 (2018).
[12]C. L. Garrido Alzar, H. Perrin, B. M. Garraway, and V. Lorent, Phys. Rev. A **74**, 053413 (2006).
[13]C. M. Wilson, T. Duty, F. Persson, M. Sandberg, G. Johansson, and P. Delsing, Phys. Rev. Lett. **98**, 257003 (2007).
[14]S. N. Shevchenko, A. I. Ryzhov, and F. Nori, Phys. Rev. B **98**, 195434 (2018).
[15]M. Bonifacio, D. Domínguez, and M. J. Sánchez, Phys. Rev. B **101**, 245415 (2020).
[16]C. Kenfack-Sadem, C. M. Ekengoue, J. E. Danga, A. J. Fotue, M. F. C. Fobasso, and L. C. Fai, Eur. Phys. J. Plus **135**, 815 (2020).
[17]A. Sokolova, G. Fedorov, E. Il'ichev, and O. Astafiev, Phys. Rev. A **103**, 013718 (2021).
[18]M. A. Antón, S. Maede-Razavi, F. Carreño, I. Thanopulos, and E. Paspalakis, Phys. Rev. A **96**, 063812 (2017).
[19]G. Bevilacqua, V. Biancalana, A. Vigilante, T. Zanon-Willette, and E. Arimondo, Phys. Rev. Lett. **125**, 093203 (2020).
[20]D. Pitsun, A. Sultanov, I. Novikov, E. Mutsenik, B. Ivanov, A. Matanin, V. Polozov, E. Malevannaya, A. Ivanov, G. Fedorov, K. Delfanazari, I. Rodionov, and E. Il'ichev, Phys. Rev. Appl. **14**, 054059 (2020).
[21]A. N. Omelyanchouk, S. N. Shevchenko, Y. S. Greenberg, O. Astafiev, and E. Il'ichev, Fiz. Nizk. Temp. **36**, 1117 (2010) [Low Temp. Phys. **36**, 893 (2010)].
[22]S. N. Shevchenko, G. Oelsner, Y. S. Greenberg, P. Macha, D. S. Karpov, M. Grajcar, U. Hubner, A. N. Omelyanchouk, and E. Il'ichev, Phys. Rev. B **89**, 184504 (2014).
[23]G. Y. Kryuchkyan, V. Shahnazaryan, O. V. Kibis, and I. A. Shelykh, Phys. Rev. A **95**, 013834 (2017).
[24]D. S. Karpov, G. Oelsner, S. N. Shevchenko, Y. S. Greenberg, and E. Il'ichev, Fiz. Nizk. Temp. **42**, 246 (2016) [Low Temp. Phys. **42**, 189 (2016)].
[25]Y.-J. Zhao, J.-H. Ding, Z. H. Peng, and Y.-. Liu, Phys. Rev. Appl. **95**, 043806 (2017).
[26]P. Neilinger, S. N. Shevchenko, J. Bogár, M. Rehák, G. Oelsner, D. S. Karpov, U. Hübner, O. Astafiev, M. Grajcar, and E. Il'ichev, Phys. Rev. B **94**, 094519 (2016).
[27]G. Oelsner, U. Hübner, and E. Il'ichev, Phys. Rev. B **101**, 054511 (2020).
[28]S. N. Shevchenko and D. S. Karpov, Phys. Rev. Appl. **10**, 014013 (2018).
[29]K. Koshino, H. Terai, K. Inomata, T. Yamamoto, W. Qiu, Z. Wang, and Y. Nakamura, Phys. Rev. Lett. **110**, 263601 (2013).
[30]J.-C. Besse, S. Gasparinetti, M. C. Collodo, T. Walter, P. Kurpiers, M. Pechal, C. Eichler, and A. Wallraff, Phys. Rev. X **8**, 021003 (2018).
[31]S. Kono, K. Koshino, Y. Tabuchi, A. Noguchi, and Y. Nakamura, Nat. Phys. **14**, 546 (2018).
[32]S. Kohler, Phys. Rev. A **98**, 023849 (2018).
[33]M. Silveri, J. Tuorila, M. Kemppainen, and E. Thuneberg, Phys. Rev. B **87**, 134505 (2013).
[34]C. Kurter, P. Tassin, L. Zhang, T. Koschny, A. P. Zhuravel, A. V. Ustinov, S. M. Anlage, and C. M. Soukoulis, Phys. Rev. Lett. **107**, 043901 (2011).

Translated by AIP Author Services